Available online at www.sciencedirect.com
ScienceDirect
Ocean Engineering 34 (2007) 185–191
OCEAN ENGINEERING
www.elsevier.com/locate/oceaneng

Long wave reflection from submerged trapezoidal breakwaters

Hsien-Kuo Chang*, Jin-Cheng Liou

Department of Civil Engineering, National Chiao Tung University, 1001 Ta Hsuech Road, Hsinchu, 300, Taiwan.

Received 6 September 2005; accepted 1 November 2005
Available online 19 April 2006

Abstract

This study addresses the reflection and transmission of long waves from a trapezoidal breakwater and a series of trapezoidal breakwaters, using the matching method. A systematic shape transfer is derived to determine wave reflection and transmission. The peak Bragg reflection of long waves from a series of trapezoidal breakwaters is shifted toward low frequency. In spite of the spacing between any pair of breakwaters, the top plane width and the arrangement of the series of breakwaters are found to be the two major parameters in designing multiply composite Bragg breakwaters.

Keywords: Wave reflection; Bragg reflection; Long wave

1. Introduction

Submerged breakwaters and artificial reefs have become increasingly common as devices for protecting against coastal erosion, because they are effective but have minimal visual impact. Many submerged trapezoidal breakwaters are built in shallow water regions where most waves are long waves. Chang and Liou (2004) attempted to clarify the simple problem of propagation of long waves over a sloping step, and addressed the extent to which the face slope of the step affects reflection and transmission of the waves. This investigation applies Chang and Liou's (2004) matching method to elucidate the reflection and transmission of long waves from a trapezoidal breakwater. Reflection from a series of trapezoidal breakwaters is also discussed, following the work on artificial Bragg breakwaters by Kirby and Aonton (1990).

Bragg resonance, which was first identified in crystallography, between the surface waves and the sand ripples occurs under the particular condition in which the bar spacing is about half of the wavelength of normally incident waves. The mechanisms of resonant Bragg reflection and the non-resonant reflection of water waves are examined by several theoretical analyses and numerical simulations (Heathershaw, 1982; Davies, 1982; Davies and Heathershaw, 1984; Mei, 1985; Kirby, 1986; Dalrymple and Kirby, 1986; Hara and Mei, 1987; Mattioli, 1991).

Bailard et al. (1992) used a staggered nine-element bar field to reduce the volume erosion by 25% along beaches on the US Gulf coast and the Atlantic coast. Their numerical results reveal that the bandwidths of primary and higher-order harmonic resonances are narrow. Therefore, Bailard et al. (1992) determined that the application of a Bragg breakwater might be practically limited on most US beaches. Hsu et al. (2002) studied the effect of the shape of artificial breakwaters on the Bragg reflection in practical cases. It is interesting to note that in the case with a bottom comprising a superposition of two or more sinusoids with different wave numbers, higher-order harmonic Bragg resonances occur at higher frequencies and subharmonic Bragg resonances occur at low frequency. Guazzelli et al. (1992), O'Hare and Davies (1993), Cho and Lee (2000) and Hsu et al. (2003) proved the existence of higher-order harmonic and subharmonic Bragg resonances. Hsu et al. (2003) used multiply composite artificial bars to obtain high Bragg reflections for engineering purposes.

The rest of this paper is organized as follows. Sections 2 and 3 derive a systematically shaped transfer to determine the reflection and transmission of long waves propagating over a trapezoidal breakwater, and a series of trapezoidal breakwaters, respectively. Section 4.1 compares the wave

*Corresponding author. Fax: 886 3 5131487.
E-mail address: hkc@faculty.nctu.edu.tw (H.-K. Chang).

0029-8018/$ - see front matter © 2006 Elsevier Ltd. All rights reserved.
doi:10.1016/j.oceaneng.2005.11.017

reflections obtained by the method herein with those obtained by Mei (1983) and Miles (1981). In Section 4.2, the peak Bragg reflection, shifted downward in low frequency, is found by the proposed method and its physical meaning is explained. The analysis indicates that the width of the top plane and the arrangement of a series of breakwaters are two other key parameters in the design of multiply composite Bragg breakwaters for practical use. Conclusions are finally drawn in Section 5.

2. The solutions for a submerged trapezoidal breakwater

Considering wave reflection by a trapezoidal submerged breakwater, as shown in Fig. 1, the x-axis positively points in wave incident direction and is set on the mean water depth. The original coordinate system is set at the toe of the ascending slope of a submerged breakwater and B_2 denotes the width of the top plane. Water depths at horizontal bottom are represented by h_1, h_2, and h_3, for regions I, III and V, respectively.

The governing equations for long waves are in terms of vertically depth integrated continuity equation and equations of motion. For the case of depth varying configuration, the one-dimensional linearized equation of motion is written in the form (Mei 1983, pp.135)

$$gh\frac{\mathrm{d}^2\eta}{\mathrm{d}x^2}+g\frac{\mathrm{d}h}{\mathrm{d}x}\frac{\mathrm{d}\eta}{\mathrm{d}x}+\sigma^2\eta=0, \tag{1}$$

where η is the surface elevation; $\sigma=2\pi/T$ is the wave frequency in which T is the wave period; g is the gravitational acceleration, and h is the water depth that varies on the sloping plane. As linear long waves are considered, all periodic physical quantities can be expressed as a function multiplied by $\exp(-\mathrm{i}\sigma t)$ where $\mathrm{i}=\sqrt{-1}$ is the unit imaginary number.

If the depth is constant, the second term on the left-hand of Eq. (1) thus vanishes and Eq. (1) becomes one-dimensional wave equation of which the solution is

$$\eta=A_i\mathrm{e}^{\mathrm{i}k_ix}+B_i\mathrm{e}^{-\mathrm{i}k_ix}, \tag{2}$$

where $k_i=\sigma/\sqrt{gh_i},(i=1,3,5)$ is the wave number; A_i and B_i are the wave amplitudes to be determined by boundary conditions. The first term on the right-hand side of Eq. (2) represents a wave that propagates from the right to the left and the second term denotes a reflected wave propagating in opposite direction.

When the face slope is considered in Eq. (1) introducing a new variable $X=h=h_1-x\tan\beta$ where $\tan\beta$ is the face slope of the breakwater yields

$$X\frac{\mathrm{d}^2\eta}{\mathrm{d}X^2}+\frac{\mathrm{d}\eta}{\mathrm{d}X}+n\eta=0 \tag{3}$$

and

$$n=\frac{\sigma^2}{g\tan^2\beta}. \tag{4}$$

Eq. (3) is a second-order differential equation which can be transformed into a typical Bessel equation. Thus, the corresponding solution for regions II and IV is given in terms of Bessel functions as follows

$$\eta=AJ_0(2\sqrt{nX})+BY_0(2\sqrt{nX}), \tag{5}$$

where J_0 and Y_0 are the Bessel function of the first kind and the second kind, respectively, of order zero; A and B are the undetermined constants. Eq. (5) was ready derived by Dean (1964), Miles (1990) and Dingemans (1997).

The water surface elevation and its first derivative should be continuous at the junctions between the successive regions due to the conservations of both mass and momentum to have the governing equations in a matrix form as follows:

for regions I and II:

$$\begin{pmatrix}1 & 1\\ \mathrm{i}k_1 & -\mathrm{i}k_1\end{pmatrix}\begin{pmatrix}1\\ R\end{pmatrix}=\begin{pmatrix}J_0(2\sqrt{n_{12}h_1}) & Y_0(2\sqrt{n_{12}h_1})\\ J_0'(2\sqrt{n_{12}h_1}) & Y_0'(2\sqrt{n_{12}h_1})\end{pmatrix}\begin{pmatrix}A_{\mathrm{I-II}}\\ A_{\mathrm{I-II}}\end{pmatrix} \tag{6}$$

for regions II and III:

$$\begin{pmatrix}J_0(2\sqrt{n_{12}h_1}) & Y_0(2\sqrt{n_{12}h_1})\\ J_0'(2\sqrt{n_{12}h_1}) & Y_0'(2\sqrt{n_{12}h_1})\end{pmatrix}\begin{pmatrix}A_{\mathrm{I-II}}\\ A_{\mathrm{I-II}}\end{pmatrix}=\begin{pmatrix}1 & 1\\ \mathrm{i}k_2 & -\mathrm{i}k_2\end{pmatrix}\begin{pmatrix}A_{\mathrm{II-III}}\\ A_{\mathrm{II-III}}\end{pmatrix} \tag{7}$$

for regions III and IV:

$$\begin{pmatrix}\mathrm{e}^{\mathrm{i}k_2B_2} & \mathrm{e}^{-\mathrm{i}k_2B_2}\\ \mathrm{i}k_2\mathrm{e}^{\mathrm{i}k_2B_2} & -\mathrm{i}k_2\mathrm{e}^{-\mathrm{i}k_2B_2}\end{pmatrix}\begin{pmatrix}A_{\mathrm{II-III}}\\ B_{\mathrm{II-III}}\end{pmatrix}=\begin{pmatrix}J_0(2\sqrt{n_{23}h_2}) & Y_0(2\sqrt{n_{23}h_2})\\ J_0'(2\sqrt{n_{23}h_2}) & Y_0'(2\sqrt{n_{23}h_2})\end{pmatrix}\begin{pmatrix}A_{\mathrm{III-IV}}\\ B_{\mathrm{III-IV}}\end{pmatrix} \tag{8}$$

for regions IV and V:

$$\begin{pmatrix}J_0(2\sqrt{n_{23}h_3}) & Y_0(2\sqrt{n_{23}h_3})\\ J_0'(2\sqrt{n_{23}h_3}) & Y_0'(2\sqrt{n_{23}h_3})\end{pmatrix}\begin{pmatrix}A_{\mathrm{III-IV}}\\ B_{\mathrm{III-IV}}\end{pmatrix}=\begin{pmatrix}1\\ \mathrm{i}k_3\end{pmatrix}T. \tag{9}$$

Applying matrix multiplication to Eqs. (6)–(9) leads to the following expression:

$$\begin{pmatrix}1\\ R\end{pmatrix}=\mathbf{H}_i\mathbf{S}_2\mathbf{W}_3\mathbf{S}_4\mathbf{H}_tT=\begin{pmatrix}c_{11}\\ c_{21}\end{pmatrix}T, \tag{10}$$

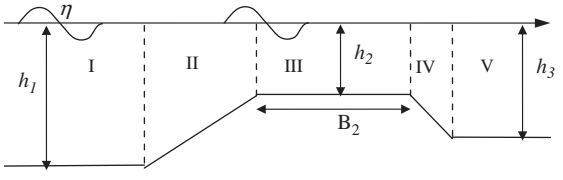

Fig. 1. Definition sketch of a trapezoidal submerged breakwater.

where

$$\mathbf{H}_i = \begin{pmatrix} 1 & 1 \\ \mathrm{i}k_1 & -\mathrm{i}k_1 \end{pmatrix}^{-1} = \frac{1}{2}\begin{pmatrix} 1 & -\frac{\mathrm{i}}{k_1} \\ 1 & \frac{\mathrm{i}}{k_1} \end{pmatrix}, \tag{11a}$$

$$\mathbf{S}_2 = \begin{pmatrix} J_0\left(2\sqrt{n_{12}h_1}\right) & Y_0\left(2\sqrt{n_{12}h_1}\right) \\ J_0'\left(2\sqrt{n_{12}h_1}\right) & Y_0'\left(2\sqrt{n_{12}h_1}\right) \end{pmatrix} \begin{pmatrix} J_0\left(2\sqrt{n_{12}h_2}\right) & Y_0\left(2\sqrt{n_{12}h_2}\right) \\ J_0'\left(2\sqrt{n_{12}h_2}\right) & Y_0'\left(2\sqrt{n_{12}h_2}\right) \end{pmatrix}^{-1}, \tag{11b}$$

$$\mathbf{W}_3 = \begin{pmatrix} 1 & 1 \\ \mathrm{i}k_2 & -\mathrm{i}k_2 \end{pmatrix} \begin{pmatrix} \mathrm{e}^{\mathrm{i}k_2B_2} & \mathrm{e}^{-\mathrm{i}k_2B_2} \\ \mathrm{i}k_2\mathrm{e}^{\mathrm{i}k_2B_2} & -\mathrm{i}k_2\mathrm{e}^{-\mathrm{i}k_2B_2} \end{pmatrix}^{-1} = \begin{pmatrix} \cos k_2B_2 & -\frac{1}{k_2}\sin k_2B_2 \\ k_2\sin k_2B_2 & \cos k_2B_2 \end{pmatrix}, \tag{11c}$$

$$\mathbf{S}_4 = \begin{pmatrix} J_0(2\sqrt{n_{23}h_2}) & Y_0(2\sqrt{n_{23}h_2}) \\ J_0'(2\sqrt{n_{23}h_2}) & Y_0'(2\sqrt{n_{23}h_2}) \end{pmatrix} \begin{pmatrix} J_0(2\sqrt{n_{23}h_3}) & Y_0(2\sqrt{n_{23}h_3}) \\ J_0'(2\sqrt{n_{23}h_3}) & Y_0'(2\sqrt{n_{23}h_3}) \end{pmatrix}^{-1}, \tag{11d}$$

$$\mathbf{H}_t = \begin{pmatrix} 1 \\ \mathrm{i}k_3 \end{pmatrix}. \tag{11e}$$

Both $\mathbf{H}_i$ and $\mathbf{H}_t$, called radiation transfers hereafter, indicate the waves radiating at the ends of infinite horizontal beds. $\mathbf{S}_2$ and $\mathbf{S}_4$ display the slope effect on wave reflection and transmission so that we call them slope transfer. The former represents a wave traveling up from the deep region to the shallow region and the latter indicating a wave going down from the shallow region to the deep region. If a trapezoidal breakwater is symmetrical the slope face and water depths of both sides are the same and then have $n_{12} = n_{23}$ and $h_1 = h_3$. Comparing Eq. (11b) and Eq. (11d) thus yields $\mathbf{S}_4 = \mathbf{S}_2^{-1}$ for a symmetrical trapezoidal breakwater. Finally, $\mathbf{W}_3$ is the width transfer showing waves propagating over a finite horizontal plane.

Eq. (10) indicates the resultant wave reflection and transmission through a sequence of radiation transfer, slope transfer and width transfer of an incident wave passing over a submerged trapezoidal breakwater. The resultant transfers constitute a shape transfer. Matrix multiplication in Eq. (10) finally gives a dimension of 2×1 matrix, and transmission and reflection coefficients are easily obtained as follows:

$$T = \frac{1}{c_{11}} \tag{12}$$

and

$$R = \frac{c_{21}}{c_{11}}. \tag{13}$$

When the face slope of a breakwater is neglected, the depth changes discontinuity at the junctions. Considering the simple case, Mei (1983) related the water surface elevation and mass flux across the discontinuity to identify the reflected and the transmitted waves. The reflection and transmission coefficients are presented in a simple form

$$R_{\mathrm{Mei}} = \left|\frac{(1-s_{12})(1+s_{32})\mathrm{e}^{-\mathrm{i}k_2B_2} + (1+s_{12})(1-s_{32})\mathrm{e}^{\mathrm{i}k_2B_2}}{(1+s_{12})(1+s_{32})\mathrm{e}^{-\mathrm{i}k_2B_2} - (1-s_{12})(1-s_{32})\mathrm{e}^{\mathrm{i}k_2B_2}}\right|, \tag{14}$$

and

$$T_{\mathrm{Mei}} = \left|\frac{4s_{12}}{(1+s_{12})(1+s_{32})\mathrm{e}^{-\mathrm{i}k_2B_2} - (1-s_{12})(1-s_{32})\mathrm{e}^{\mathrm{i}k_2B_2}}\right|, \tag{15}$$

where the substitutions $s_{ij} = k_ih_i/k_jh_j$ $(i, j = 1, 2, 3)$ denote the relative water depth.

Miles (1981) applied finite Fourier cosine transform to solve the problem of a wave reflected by an obstacle with small and continuous height variation and derived the wave reflection and transmission coefficients. Kirby and Anton (1990) extended Miles' theory to the situation of a mildly sloping bottom with rapidly varying but small-amplitude undulation. The expressions for reflection and transmission coefficients derived by Miles (1981) are written as

$$R_{\mathrm{Miles}} = \left|\frac{2k^2}{2kh + \sinh 2kh}\int_{-\infty}^{\infty}\delta(x)\mathrm{e}^{2\mathrm{i}kx}\mathrm{d}x\right| \tag{16}$$

and

$$T_{\mathrm{Miles}} = \left|1 + \mathrm{i}\frac{2k^2}{2kh + \sinh 2kh}\int_{-\infty}^{\infty}\delta(x)\mathrm{d}x\right|, \tag{17}$$

where $\delta(x)$ is the shape function of the obstacle of which the height is measured from the horizontal bottom. Neglecting the effect of depth variation on the wave number in the integrals of Eqs. (16) and (17) associated with the shape of a trapezoidal breakwater produces

$$R_{\mathrm{Miles}} = \frac{1}{2(2kh + \sinh 2kh)}\left|\begin{array}{l} -2\mathrm{i}\mathrm{e}^{2\mathrm{i}kL_2}(-1+\mathrm{e}^{2\mathrm{i}kB_2})(h_1-h_2)k \\ +\frac{h_1-h_2}{L_2}(-1+\mathrm{e}^{2\mathrm{i}kL_2} - 2\mathrm{i}\mathrm{e}^{2\mathrm{i}kL_2}kL_2) \\ +\frac{\mathrm{e}^{2\mathrm{i}k(L_2+B_2)}(h_2-h_3)}{L_4}(1-\mathrm{e}^{2\mathrm{i}kL_4} \\ +2\mathrm{i}k\left[(-1+\mathrm{e}^{2\mathrm{i}kL_4})(L_2+B_2) + \mathrm{e}^{2\mathrm{i}kL_4}L_4\right] \end{array}\right| \tag{18}$$

and

$$T_{\mathrm{Miles}} = \left|1 + \frac{\mathrm{i}}{2}\frac{2k^2}{2kh + \sinh 2kh}[h_1(L_2+2B_2) + h_2(L_2+L_4) - h_3(2L_2+2B_2+L_4)]\right| \tag{19}$$

where $k = \sigma/\sqrt{gh_m}$ is the mean wave number in which h_m is the mean water depth.

3. The solutions for a series of submerged trapezoidal breakwaters

A series of N sets of submerged trapezoidal breakwaters over a horizontal bed is plotted in Fig. 2. The width at the bottom plane between two breakwaters is B_1.

The region V at the bottom plane between two breakwaters is finite which is similar to the region III at the top plane. Thus the wave in the region V propagates in a similar way to that in the region III. The effect of a finitely horizontal bottom plane on wave reflection and transmission can be expressed by a width transfer alike Eq. (11c) having the form

$$\mathbf{W}_5 = \begin{pmatrix} \cos k_1 B_1 & -\frac{1}{k_1}\sin k_1 B_1 \\ k_1 \sin k_1 B_1 & \cos k_1 B_1 \end{pmatrix}. \tag{20}$$

Following the procedure mentioned in the above section, the wave reflection and transmission from a series of breakwaters can be related and equated by

$$\begin{aligned} \begin{pmatrix} 1 \\ R \end{pmatrix} &= \mathbf{H}_i \overbrace{\mathbf{S}_2\mathbf{W}_3\mathbf{S}_4\mathbf{W}_5\mathbf{S}_2\mathbf{W}_3\mathbf{S}_4\mathbf{W}_5\cdots}^{N-1}\mathbf{S}_2\mathbf{W}_3\mathbf{S}_4\mathbf{H}_t T \\ &= \mathbf{H}_i[\mathbf{S}_2\mathbf{W}_3\mathbf{S}_4\mathbf{W}_5]^{N-1}\mathbf{S}_2\mathbf{W}_3\mathbf{S}_4\mathbf{H}_t T. \end{aligned} \tag{21}$$

A sequence of matrix multiplication is accomplished on the right hand side of Eq. (21) and then two equations are available to solve wave reflection and transmission coefficients.

4. Results and discussions

4.1. Single breakwater

Two computational conditions are specified for determining the reflection and transmission of a wave propagating over a single breakwater by the proposed method. The conditions for case one are $h_1 = h_3 = 2.4\,\text{m}$, $h_2 = 0.8\,\text{m}$, $L_2 = 3.2\,\text{m}$, $B_2 = 4\,\text{m}$, $L_4 = 2.4\,\text{m}$ and $T = 10\,\text{s}$. In the other case, the only difference is $h_3 = 1.6\,\text{m}$ instead of 2.4 m in order to make the bottom depth different at both ends. The relative water depth, defined as the ratio of the water depth to the wavelength, at the ends is 1/19.9, which value is regarded as shallow water area for long wave propagation. These computational conditions are often applied in the practical design of submerged breakwaters. Table 1 presents the obtained reflection and transmission coefficients.

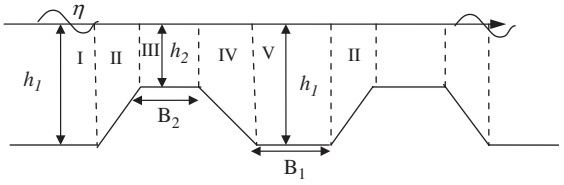

Fig. 2. Definition sketch of a series of trapezoidal submerged breakwaters.

In case one, the proposed method and Mei (1983) both have a value of $R^2 + T^2 = 1$, which represents the conservation of energy flux. The wave transmission evaluated by Eq. (17) definitely exceeds unity. Hence, the formula of Miles (1981) fails to conserve energy flux. However, the wave reflection obtained by Eq. (18) slightly exceeds that obtained by the proposed method, by 0.05. The reflection coefficient calculated by the proposed method is slightly higher than that of Mei (1983) by 0.06.

In case 2, all results demonstrate that $R^2 + T^2 > 1$, because the depth of the bottom differs at the ends. The proposed method predicts a higher wave reflection coefficient than Mei (1983). The transmission coefficient calculated by the method proposed herein is 0.023 lower than that of Mei (1983).

The energy flux is defined as the wave energy times the group velocity, where the wave energy is $\rho g H^2/8$, and ρ is the density of water and H is the wave height. According to linear wave theory, the group velocity is $\sqrt{gh}$ in shallow water region. The energy flux in one direction must be conserved through any two cross sections. Equating the energy fluxes in regions III and V yields,

$$(1 - R^2)\frac{\rho g H_1^2}{8}\sqrt{gh_1} = \frac{\rho g H_3^2}{8}\sqrt{gh_3}, \tag{22}$$

where H_1 represents the wave height at h_1 and H_3 is the wave height at h_3. Accordingly, the transmission coefficient is

$$T = \frac{H_3}{H_1} = \left[(1 - R^2)\sqrt{\frac{h_1}{h_3}}\right]^{1/2} \tag{23}$$

Substituting $R = 0.3967$ and $h_1/h_3 = 1.5$ into Eq. (23) yields $T = 1.0159$, which is the same value as that obtained using Eq. (12) and presented in Table 1. The shoaling effect yields a transmission coefficient of greater than unity.

Table 1
A comparison of the reflection and transmission coefficients obtained by the present method, Mei (1983) and Miles (1981)

Author/equation used	Case 1			Case 2		
	R	T	R^2+T^2	R	T	R^2+T^2
Chang/Eq. (13), (12)	0.4724	0.8814	1.0000	0.3967	1.0159	1.1894
Mei/Eq. (14), (15)	0.4113	0.9115	1.0000	0.3449	1.0388	1.1980
Miles/Eq. (18), (19)	0.5227	1.0092	1.2917	0.3579	1.0062	1.1132

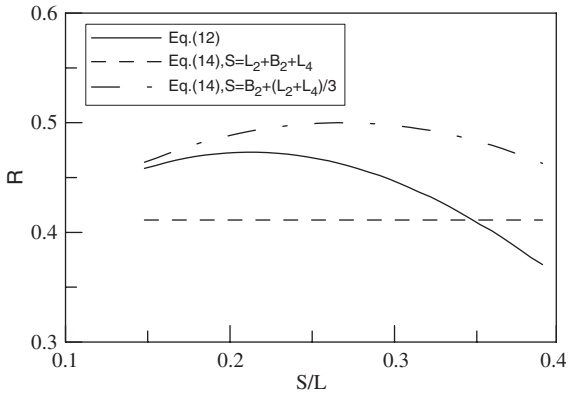

Fig. 3. Reflection coefficients for a wave over a trapezoidal breakwater with various sloping faces but with a fixed top width.

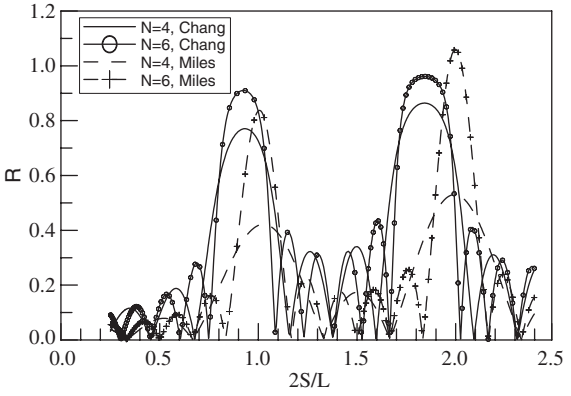

Fig. 4. Wave reflection from sets of different numbers of breakwaters, using the proposed method and Miles method.

If the slope of the sloping face varies, but the width of the top plane is fixed, then the calculated reflection coefficients of a wave with a period of 10 s are as plotted in Fig. 3. The depth of the water at each part of a breakwater is the same as in case 1; the step is fixed at a height of 1.6 m. The face slope on the ascending side varies from 1 to 1/8 and that on the leeward side varies from one to 1/3.5. The spacing between the two breakwaters is defined as $S = L_2 + B_2 + L_4$. Fig. 3 reveals that the reflection obtained by Eq. (14), and denoted by a dashed line is a constant of 0.4113, because a breakwater has a fixed height, and that the proposed method yields the reflection denoted by a solid line with a maximum value of 0.4731 at $S/L = 0.21$. The triangular parts of a breakwater on both sides are deformed into a rectangular shape with an equivalent area. Therefore, $(L_2 + L_4)/3$ is added to the original top width of a breakwater so the corrected top width is $B_2 + (L_2 + L_4)/3$. According to the corrected top width of the breakwater, the reflection coefficient obtained by Eq. (14), represented by the broken line in Fig. 3, exceeds that obtained by the proposed method, reaching a maximum value of 0.5000 at $S/L = 0.266$.

4.2. Multiply composite breakwaters

Substituting the shape of each breakwater into the undulation in Eq. (16) and integrating it for each of a series of N sets of breakwaters, yields a resultant wave reflection. Fig. 4 compares the wave reflection from a series of N sets of symmetrical breakwaters using the proposed method with that obtained by Miles' method. The shape of each breakwater is given by $h_1 = 2.4$ m, $h_2 = 1.2$ m, $L_2 = L_4 = 2.4$ m, $B_2 = 4$ m; the spacing between the two breakwaters $B_1 = 20$ m is fixed, and $N = 4$ or 6 is used in the computation. In practical engineering design, a breakwater face slope of 1:2 is commonly used.

Miles' result shows that the peak amplitude of Bragg reflection increases quickly and the bandwidth falls as the number of breakwaters rises. However, Fig. 4 depicts a slow increase in the peak amplitude of the Bragg reflection and a slow decline in the bandwidth obtained by the proposed method. The peak Bragg reflection obtained by Miles' method occurs exactly at $2S/L = 1$ and 2. An interesting finding of the proposed method is that the peak Bragg reflection shifts toward $2S/L \approx 0.93$, and 1.84, respectively, which are lower than Miles' values. According to the original Bragg law in optics and Miles' theory for wave Bragg reflection, the peak Bragg reflection occurs exactly at $2S/L = 1$ and 2, based on the assumption that the speed of propagation of a wave remains constant. Variation in the wave celerity with water depth is considered, so the wave has a shorter wavelength and moves more slowly in the ridge region because the water is shallower there than it is in the flat bottom plane. When an incident wave travels for a distance $S = L/2$ and then the reflected wave returns for the same distance, both waves are in phase and form an envelope. In this situation in which Bragg reflection occurs, the envelope has a maximum amplitude at anti-nodes and minimum amplitude at nodes. If the spacing between the two breakwaters is fixed, then a wave with a constant wavelength of $L = 2S$ is required to satisfy Bragg's law. A longer wave is required to compensate for phase loss because the wave is slower in the shallow region than in the deep region. Therefore, this method, accounting for the variation of the wavelength with the depth of water, reveals downward shift in the frequency of the peak Bragg reflection.

The peak Bragg reflection at $2S/L = 2$, obtained by Miles' method, is 1.06, which is greater than one. This unexpected finding indicates the neglect of the necessary variations in wavenumber with the change in water depth. As stated above, the proposed method conserves energy such that the sum of the squares of the transmission coefficient and the reflection coefficient is unity. Thus, the reflection coefficient obtained by the proposed method never exceeds unity.

The space between the two breakwaters is a key parameter in determining Bragg reflection. The effect of the width of a top plane on wave reflection when the spacing between two breakwaters is fixed, is discussed. Fig. 5 displays the results. The computational conditions of Fig. 4 involve $N = 4$, but two other cases with (B_1, B_2)

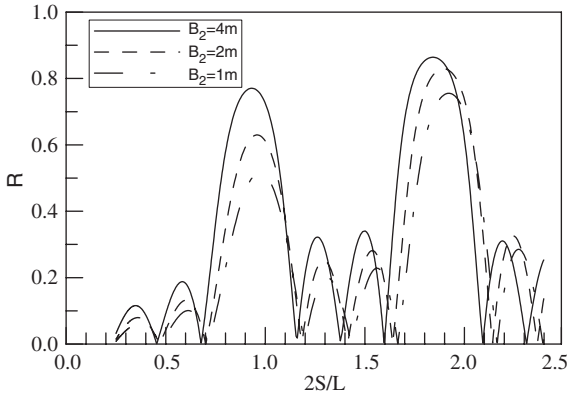

Fig. 5. Wave reflection from a series of breakwaters with top planes of various widths.

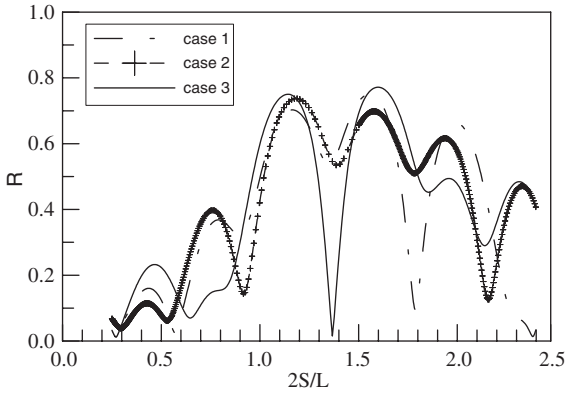

Fig. 6. Wave reflection from a series of breakwaters in cases 1–3.

Table 2
Three kinds of different arrangement of multiply composite breakwaters examined

Case	B1-1 (m)	B1-2 (m)	B1-3 (m)
Case 1	20	12	8
Case 2	12	8	20
Case 3	8	20	12

values of (22 m, 2 m) and (23 m, 1 m) are considered. Fig. 5 demonstrates that the width of a top plane influences wave reflection especially near $2S/L = 1$ and the downshift in the peak Bragg reflection is larger from a larger top plane. Accordingly, the width of a top plane becomes important in designing wave Bragg reflection.

Guazzelli et al. (1992), and Hsu et al. (2003) investigated two combinations of multiply composite bars. They found that the bandwidth of Bragg reflection can be improved using multiply composite bars, and the number of the bars, and spacing between them, are key parameters that lead to optimal and variable Bragg reflection. They divided their multiply composite bars into two groups. The bars were equally spaced in both groups. If the shape of the bars and the spacing between two bars are fixed, whether the Bragg reflection depends on the arrangement of the bars is an interesting question. Four breakwaters whose shapes are specified by $h_1 = 2.4$ m, $h_2 = 1.2$ m, $L_2 = L_4 = 2.4$ m, $B_2 = 4$ m are separated by three spaces of 8, 12 and 20 m. Table 2 specifies three arrangement of these composite breakwaters. Fig. 6 plots the wave reflection obtained by the proposed method from the multiply composite breakwater in cases 1–3. Fig. 6 presents the wave reflections in these three cases. The reflection is minimum, with a value of 0.1, near $2S/L \approx 1.78$ in case 1. In case 3, the minimum wave reflection is extremely low, 0.015, near $2S/L \approx 1.37$. In the $2S/L$ range between unity and two, the wave reflection always exceeds 0.5 in case 2. This finding verifies that, in practical engineering, multiply composite breakwaters designed as in case 2 can provide high wave reflection matching, meeting the design requirements to handle waves with large periods in the real sea. In contrast, when a wave with a period of 8.68 s has $2S/L \approx 1.37$ as in case 3, its reflection coefficient is 0.015, so the design requirement of high wave reflection is not met. A favorable arrangement of multiply composite breakwaters helps to ensure the high Bragg reflection of waves with large periods.

5. Conclusions

Chang and Liou's (2004) matching method is used to determine the reflection and transmission of long waves from a trapezoidal breakwater and a series of trapezoidal breakwaters. Shape transfer, including radiation transfer, width transfer and slope transfer, are derived as a pair of equations to determine the reflection and transmission of long waves from a trapezoidal breakwater. The proposed method incorporates the conservations of both energy flux and mass, yielding more reasonable reflections than those obtained by Miles' (1981) method. Mei's (1983) method, using a corrected top width of a breakwater based on an equivalent area to the triangular parts of a trapezoidal breakwater, yields a wave reflection that differs slightly from that obtained by the proposed approach.

The peak Bragg reflection of long waves from a series of trapezoidal breakwaters obtained herein is found to be shifted toward low frequency. The phenomenon is clarified by the variation in phase loss with the wavelength, caused by a variation in water depth on the sloping face and the top plane of the breakwaters. Multiply composite Bragg breakwaters, providing wide bandwidths around harmonic resonances, can be applied in practical engineering. The width of the top plane and the arrangement of a series of breakwaters are two other key parameters in the design of multiply composite Bragg breakwaters.

References

Bailard, J.A., DeVries, J., Kirby, J.M., Guza, R.T., 1992. Bragg reflection breakwater: a new shore protection method. Proceedings of the 23nd International Conference Coastal Engineering, ASCE, New York, pp. 1702–1715.

Chang, H.K., Liou, J.C., 2004. Long wave reflection and transmission over a sloping step. China Ocean Engineering 18, 371–380.

Cho, Y.S., Lee, C., 2000. Resonant reflection of waves over sinusoidally varying topographies. Journal of Coastal Research 16 (3), 870–876.

Dalrymple, R.A., Kirby, J.T., 1986. Water waves over ripples. Journal of Waterways, Port, Coastal and Ocean Engineering, ASCE 112, 309–319.

Davies, A.G., 1982. On the interaction between surface waves and undulations of the seabed. Journal of Marine Research 40, 331–368.

Davies, A.G., Heathershaw, A.D., 1984. Surface propagation over sinusoidally varying topography. Journal of Fluid Mechanics 144, 419–446.

Dean, R.G., 1964. Long wave modification by linear transitions. Journal of the Waterways and Harbors Division, ASCE 90, 1–29.

Dingemans, M.W., 1997. Water Wave Propagation over Uneven Bottoms, Part 1 – Linear Wave Propagation, Word Scientific, Singapore, pp. 141-143.

Guazzelli, E., Rey, V., Belzons, M., 1992. Higher-order Bragg reflection of gravity surface waves by periodic beds. Journal of Fluid Mechanics 245, 301–317.

Hara, T., Mei, C.C., 1987. Bragg reflection of surface waves by periodic beds: theory and experiments. Journal of Fluid Mechanics 178, 221–241.

Heathershaw, A.D., 1982. Seabed-wave resonance and sand bar growth. Nature 296, 343–345.

Hsu, T.W., Chang, H.K., Tsai, L.H., 2002. Bragg reflection of waves by different shapes of artificial bars. China Ocean Engineering 16, 21–30.

Hsu, T.W., Tsai, L.H., Huang, Y.T., 2003. Bragg scattering of water wave by multiply composite artificial bars. Coastal Engineering Journal 45 (2), 235–254.

Kirby, J.T., 1986. A general wave equation for waves over rippled beds. Journal of Fluid Mechanics 162, 171–186.

Kirby, J.T., Anton, J.P., 1990. Bragg reflection of waves by artificial bars, Proceedings of the 22nd International Conference Coastal Engineering ASCE, New York, pp., 757–768

Mattioli, F., 1991. Resonant reflection of surface waves by nonsinusoidal bottom undulations. Applied Ocean Research 13, 49–53.

Mei, C.C., 1983. The Applied Dynamics of Ocean Surface Waves, Second ed. World Scientific, Singapore.

Mei, C.C., 1985. Resonant reflection of surface water waves by periodic sandbars. Journal of Fluid Mechanics 152, 315–335.

Miles, J., 1981. Oblique surface-wave diffraction by a cylindrical obstacle. Dynamics of Atmospheres and Oceans 6, 121–123.

Miles, J., 1990. Wave reflection from a gentle sloping beach. Journal of Fluid Mechanics 214, 59–66.

O'Hare, T.J., Davies, A.G., 1993. A comparison of two models for surface-wave propagation over rapidly varying topography. Applied Ocean Research 15, 1–15.